JOURNAL OF MATERIALS SCIENCE 24 (1989) 1895–1900

Thermal stability of amorphous phases in vapour-deposited binary alloy thin films of palladium with vanadium, niobium and tantalum

G. J. VAN DER KOLK, T. MINEMURA*, J. J. VAN DEN BROEK
Philips Research Laboratories, 5600 JA Eindhoven, P.O. Box 80000, The Netherlands

Binary alloys of the systems V–Pd, Nb–Pd and Ta–Pd were vapour deposited and investigated by transmission electron microscopy. The atomic fraction, x, was varied in steps of 0.1 from one pure element to the other. The range over which an amorphous phase is observed is found to increase in width going from 3d to 5d alloying element in palladium: the compositions where amorphous phases are found are $V_{1-x}Pd_x$ (x = 0.5), $Nb_{1-x}Pd_x$ (x = 0.4 to 0.6) and $Ta_{1-x}Pd_x$ (x = 0.2 to 0.6). The composition range over which a crystalline phase is found correlates well with the single-phase solid solution region close to the melting temperature in the phase diagram. Crystallization of the $V_{0.5}Pd_{0.5}$ alloy takes place at 550 K. The amorphous $Nb_{1-x}Pd_x$ (x = 0.4, 0.5) films crystallize at 850 K, whereas the amorphous Ta–Pd films crystallize between 850 and 1050 K, depending on the composition. For $Nb_{1-x}Pd_x$ (x = 0.4 to 0.5) and $Ta_{1-x}Pd_x$ (x = 0.2 to 0.6) primary crystallization takes place into an fcc phase. The second crystallization step leads to a phase with a complex structure. The result is a two-phase system. $V_{0.5}Pd_{0.5}$ and $Nb_{0.4}Pd_{0.6}$ crystallize polymorphically to an fcc solid solution. The crystallization temperatures for the compositions which display primary crystallization are higher than for the compositions which crystallize by a polymorphic reaction.

1. Introduction

The formation range and stability of amorphous metals are important for possible applications. In the case of binary amorphous alloys composed of two transition metals, it is clear that the stability of the amorphous alloys is not governed by geometric effects, as in the dense random packing of a hard spheres model, but mainly by electronic structure effects, especially when the atomic radii are similar [1]. From scattering experiments it is known that the amorphous phase is built up from structural units; see, for example, Waseda [2]. Measurements by Sakurai *et al.* [3] on the local environment of hafnium atoms in amorphous and crystalline $Cu_{0.57}Hf_{0.43}$ alloys indicate that the atomic arrangement around hafnium atoms in the amorphous phase is nearly identical with that in the crystalline phase. Therefore, we expect that to some extent a correlation can be made between properties of crystalline materials and properties of the amorphous alloys.

Recently, various attempts were made to predict the composition range of amorphous metals as well as the crystallization temperature of binary amorphous alloys. Saunders and Miodownik [4] have applied a scheme, based on a calculation of the free enthalpy curves, which makes it possible to derive the composition range of the amorphous alloys. Other approaches rely on the information contained in the phase diagram [5]. Obviously both approaches are closely related, because of the relation between the phase diagram and the free energy curves; see, for example, van den Broek and Dirks [6]. In order to test the viability of the various models, we studied the composition range over which an amorphous alloy was found by transmission electron microscopy (TEM) of thin films of the system Pd–(V, Nb, Ta). We also analysed the crystallization behaviour and crystallization temperature. The crystallization temperatures will be compared with a model given by Buschow [7] and modified versions of the model due to Weeber [8] and Barbour *et al.* [9]. Basically, the crystallization temperature of various alloys is seen to scale linearly with the formation of a volume which has the size of an atom. The underlying idea is that this volume should be available to allow atomic transport, required for crystallization.

In this paper we discuss the stability of the amorphous phase. In another article [10] metastable crystalline phases will be discussed.

2. Experimental details

Films of V–Pd, Nb–Pd and Ta–Pd were prepared by vapour deposition from electron guns on to NaCl substrates. The thickness of the films was about

Permanent address: Hitachi Research Laboratory, Hitachi, Ltd., Hitachi 319-12, Japan.

0022–2461/89 $03.00 + .12 © *1989 Chapman and Hall Ltd.*

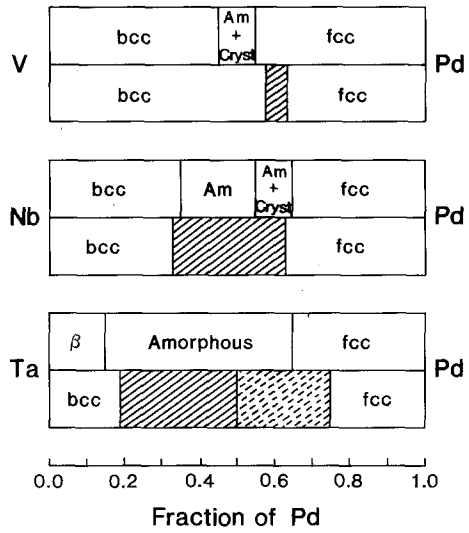

Figure 1 The composition range where amorphous phases are found as observed (upper bars), and schematically the high-temperature part of the phase diagram (lower bars). The hatched areas indicate two-phase regions or complex structures.

30 nm. The deposition rate of each element was monitored and controlled by its own quartz crystal thickness monitor. The composition of the alloys was checked with the electron microprobe, and was generally found to be within an atomic per cent of the composition as derived from the measured growth rates. The base pressure of the system was about 10^{-6} Pa. The substrate temperature was between 310 and 350 K during deposition. By dissolution of the NaCl substrate, self-supporting films were obtained, which were placed on copper or platinum grids, suitable for use in the TEM. Isochronal annealings were performed in the hot stage of the TEM, while the electron beam was switched off. The temperature was increased in steps of 50 K; at each temperature annealing was done for 15 min followed by cooling to room temperature. When crystallization was observed the temperature in between the last two annealing steps was taken as the crystallization temperature. The accuracy of the data is, therefore, not better than 25 K.

3. Results

3.1. Composition range of amorphous phases

3.1.1. V–Pd

The V–Pd system showed a bcc solid solution at vanadium-rich compositions, whereas fcc solid solutions were observed at palladium-rich compositions (see Fig. 1). Only at a composition of $V_{0.5}Pd_{0.5}$ was an amorphous phase found together with an fcc solid solution. In Fig. 2, a transmission electron micrograph is shown of the two-phase mixture. A crystalline phase had nucleated homogeneously through the film.

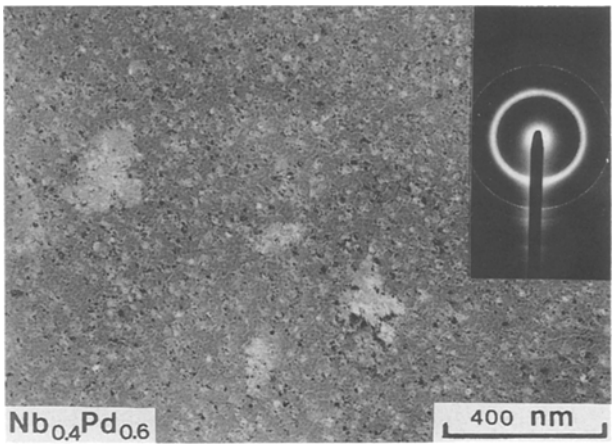

Figure 3 Transmission electron micrograph and diffraction pattern of the as-deposited system $Nb_{0.4}Pd_{0.6}$.

3.1.2. Nb–Pd

The Nb–Pd system displayed a wider composition range of amorphous phase than V–Pd. Films with compositions $Nb_{0.6}Pd_{0.4}$ and $Nb_{0.5}Pd_{0.5}$ were completely amorphous, as observed by TEM. $Nb_{0.4}Pd_{0.6}$ is composed of two phases, one of which had the fcc structure, the other was amorphous; see Fig. 3.

3.1.3. Ta–Pd

The Ta–Pd system had the largest composition range with an amorphous phase, in between $Ta_{0.8}Pd_{0.2}$ and $Ta_{0.4}Pd_{0.6}$. Mixtures of amorphous and crystalline phases were not found in this system. The various data are collected in Fig. 1.

3.2. Crystallization behaviour

3.2.1. $V_{0.5}Pd_{0.5}$

In the case of $V_{0.5}Pd_{0.5}$ crystallization of the amorphous phase just started at 525 K and was completed after annealing at 575 K. Large crystallites grew out with an fcc structure exhibiting a strong (1 1 1)

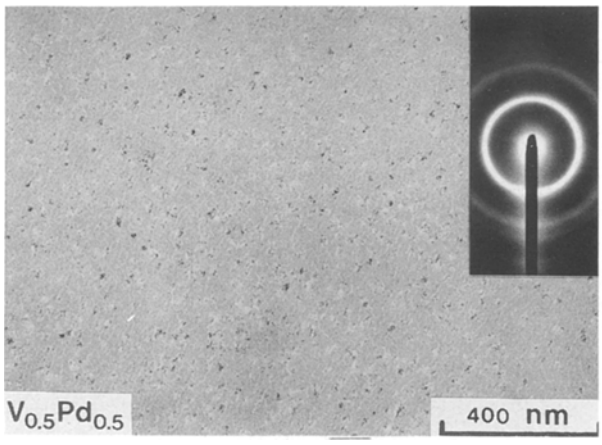

Figure 2 Transmission electron micrograph and diffraction pattern of the as-deposited system $V_{0.5}Pd_{0.5}$.

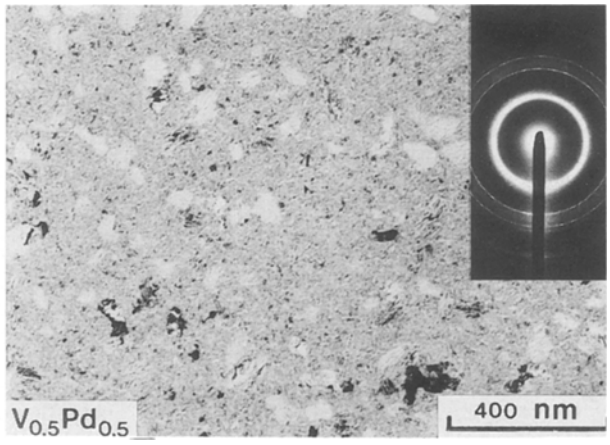

Figure 4 Transmission electron micrograph and diffraction pattern of $V_{0.5}Pd_{0.5}$ after annealing at 575 K.

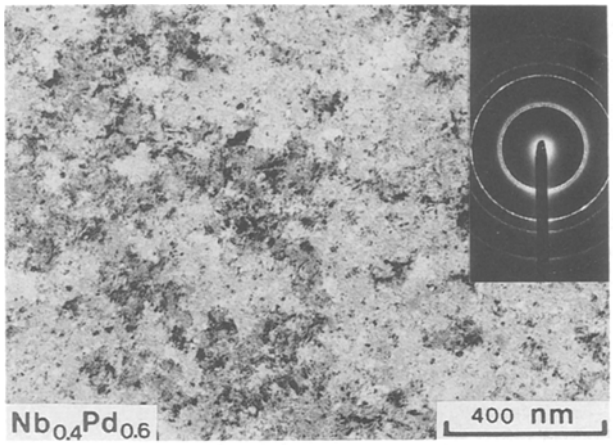

Figure 5 Transmission electron micrograph and diffraction pattern of $Nb_{0.4}Pd_{0.6}$ after annealing at 475 K.

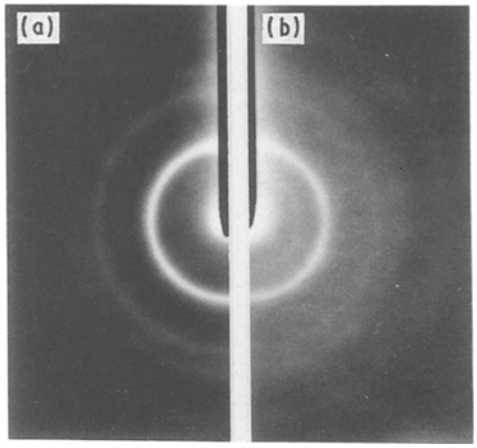

Figure 7 Diffraction pattern of $Ta_{0.6}Pd_{0.4}$ (a) as-deposited and (b) just prior to crystallization.

texture. The density of the film was homogeneous, no cracks had developed; see Fig. 4.

3.2.2. Amorphous Nb–Pd

For the amorphous Nb–Pd films, two types of crystallization behaviour were observed. $Nb_{0.4}Pd_{0.6}$ had crystallized completely after annealing at 425 K. It crystallized into an f c c solid solution, with small crystallites; see Fig. 5. $Nb_{0.5}Pd_{0.5}$ and $Nb_{0.6}Pd_{0.4}$ both crystallized between 825 and 875 K. Primary crystallization into an f c c phase took place first. The f c c crystallites were very small and again homogeneously distributed in an amorphous matrix. At slightly higher temperatures, but still in between 825 and 875 K, further crystallization took place into a σ-phase with the CrFe structure. This crystallization occurred heterogeneously: it started at places where the film was in contact with the supporting grid. Explosive crystallization occurred, leading to a structure as shown in Fig. 6.

3.2.3. Amorphous TaPd

All amorphous TaPd alloys crystallized at high temperatures, ranging from 850 K ($Ta_{0.4}Pd_{0.6}$) to 1050 K ($Ta_{0.6}Pd_{0.4}$). In the TEM it was observed that prior to crystallization something had already happened. Besides the first diffuse ring, correlated with $d = 2.2$ nm, a second very weak one developed with $d = 3.4$ nm; see Fig. 7. It is not clear whether this was caused by some structural relaxation or was due to demixing into two amorphous phases; see, for example, Duwez [11]. The temperature where this occurred was generally very close to the crystallization temperature. All compositions, even the tantalum-rich ones, showed primary crystallization into an f c c phase. The f c c particles nucleated homogeneously and were embedded in an amorphous matrix. Secondary crystallization took place at slightly higher temperatures. A complex phase formed having a diffraction pattern similar to that of the β-Ta phase as observed by Das [12] in sputtered tantalum; see Fig. 8. Various unit cells have been reported for β-Ta; see, for example [12, 13]. Essentially β-Ta consists of a superlattice, where the unit cell is composed of 27 or 64 distorted b c c unit cells. The crystallized films were preferentially oriented, so that there were not enough reflections visible to allow a unique assignment. However, the pattern can be indexed if one assumes a tetragonal unit cell similar to that found by Das, with $a/c = 0.89$ and $a = 1.08$ nm.

4. Discussion

4.1. Composition range of amorphous phases

The composition ranges of the three alloy systems where amorphous phases are found are very different.

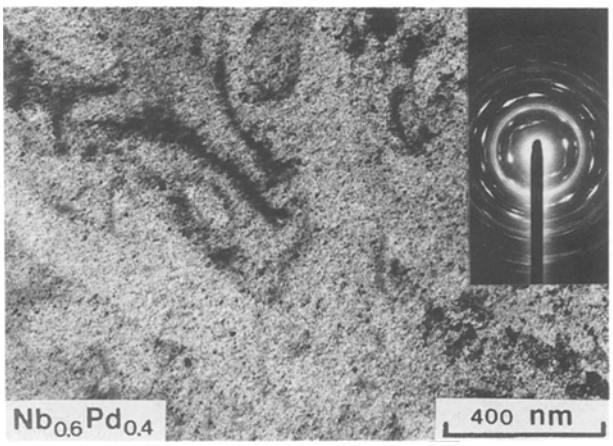

Figure 6 Transmission electron micrograph and diffraction pattern of $Nb_{0.6}Pd_{0.4}$ after annealing at 875 K.

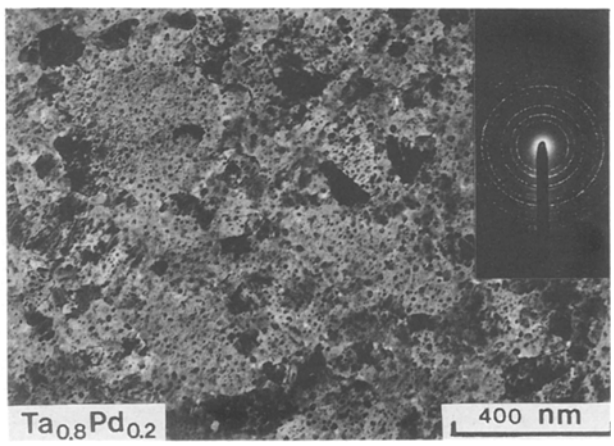

Figure 8 Transmission electron micrograph and diffraction pattern of $Ta_{0.8}Pd_{0.2}$ after annealing at 1075 K.

It is not possible to explain this simply by referring to the different atomic sizes. A vanadium atom is 10% smaller than niobium, but niobium and tantalum have the same atomic size, whereas the amorphous phase formation ranges differ by at least a factor of three in width.

This difference cannot be explained by the assumption that the formation of the crystalline phase is correlated with the surface mobility. Because the latter is related to the melting temperature, it can be expected that for the same substrate temperature, tantalum will have a lower surface mobility than vanadium and niobium. The influence of the substrate temperature on the amorphous formation range has been studied for the system Co–Zr by Samwer [14]. At a substrate temperature of 625 K no amorphous alloys are found. A gradual increase of the amorphous formation range is observed with decreasing substrate temperature. The substrate temperature of 625 K is about half the temperature of the deepest eutectic. For the systems V–Pd, Nb–Pd and Ta–Pd the substrate temperature of 300 to 350 K corresponds to, respectively, 0.21, 0.19 and 0.18 times the temperature of the deepest eutectic. Therefore it is very unlikely that the relative substrate temperature alone causes the large difference in amorphous-phase formation ranges.

It is also unlikely that the incorporation of impurities causes the large difference in amorphous formation ranges. Indeed tantalum is the most reactive of these three b c c elements. However, in the literature there is no evidence that impurities have a much stronger effect on tantalum than on niobium, with respect to the formation of amorphous phases; see, for example, Hutchinson [15] and Denbigh and Marcus [16].

The relation with the phase diagram is clearer. There is a strong correlation between the presence of a solid solution close to the melting temperature at a given composition and the formation of crystalline alloys; see, for example, Coehoorn *et al.* [17]. The opposite also holds: when the phase diagram predicts the formation of a two-phase mixture, and the two phases differ considerably in composition, long-range diffusion is required to form the equilibrium crystalline alloys. In the rapid quench during condensation, no long-range diffusion is possible, so that amorphous alloys are formed: see Fig. 1. A point of interest is the formation of complex intermetallic compounds. This definitely requires more steps than the formation of solid solutions, and the number of steps increases with increasing complexity of the structure. Watson and Bennett [18] have made a distinction between "orderly" and "disorderly" structures. A structure is called disorderly when the unit cell contains four or more inequivalent atomic sites; it is called intermediate when there are three inequivalent sites, and orderly when there are two or only one inequivalent sites. At compositions where, in our case, intermetallic compounds are stable, which are disorderly, and which persist up to the melting temperature, easy glass formation is expected according to Watson and Bennet. In the case of V–Pd, intermetallic compounds are present in the phase diagram, but only up to 400 to 500 K below the melting temperature, which means that, during rapid cooling, the metastable solid solution will form. The two-phase region at high temperatures ranges from $Pd_{0.38}V_{0.62}$ to $Pd_{0.46}V_{0.54}$. Only at a composition of $V_{0.5}Pd_{0.5}$ is an amorphous phase found; see Fig. 1.

In the case of Nb–Pd, the $NbPd_3$ phase does not persist at high temperatures. Therefore, the high-temperature two-phase region limits the expected amorphous phase formation range up to 60 at % Pd. At the niobium rich side the presence of the intermetallic compound Nb_2Pd in the phase diagram which, with five inequivalent sites, is disorderly, indicates easy glass formation up to 70 at % Nb. Amorphous phases are observed at the compositions $Nb_{0.6}Pd_{0.4}$ and $Nb_{0.4}Pd_{0.6}$.

For Ta–Pd there is a σ-phase (CrFe structure; disorderly) at a composition Ta_3Pd, which persists up to a very high temperature, and therefore easy glass formation is expected up to at least 75 at % Ta. Indeed at the composition $Ta_{0.8}Pd_{0.2}$ an amorphous phase is found. At the palladium-rich side it is less easy to predict the amorphous-phase formation range. A number of intermetallic compounds can form which are orderly (PdTa with the CuTi structure and Pd_2Ta with the $MoPt_2$ structure) or intermediate (Pd_3Ta with the Al_3Ti structure). Excluding the latter structure as favourable for glass formation yields a limitation for the amorphous phase formation range up to 50 at % Pd. When the intermediate compound Pd_3Ta is included it is 75 at % Pd. In Fig. 1 this composition region is hatched with broken lines.

The experimentally observed amorphous phase formation range is $Ta_{0.4}Pd_{0.6}$ to $Ta_{0.8}Pd_{0.2}$, which gives no clue as to whether or not we should include the intermediate structure as an indicator for easy glass formation.

4.2. Crystallization behaviour

For all amorphous alloys except $V_{0.5}Pd_{0.5}$ and $Nb_{0.4}Pd_{0.6}$, primary crystallization into an f c c phase is observed. The two exceptions crystallize polymorphically, see Köster [19], to an f c c solid solution. From the phase diagram one would expect $V_{0.5}Pd_{0.5}$ to crystallize into an f c c solid solution. The composition $Nb_{0.4}Pd_{0.6}$ is just a few atomic per cent outside the range of solid solubility. For the other alloys investigated, the equilibrium phase diagrams indicate two-phase regions. Apparently this results in primary crystallization, and in this connection it is interesting to note that the primary phase is always the f c c phase. The mobility of a specific atom in an amorphous matrix has been correlated with the enthalpy of formation of a hole with the size of that atom; see Buschow and Beekmans [20]. In our case we observed nucleation of the f c c phase first. This may suggest that palladium diffuses faster than vanadium, niobium or tantalum in the amorphous matrix. Palladium is the smaller atom, so it is expected to diffuse faster.

The temperature where diffusion occurs is predicted by Buschow's rule: $T_x = 7.5 H_v$, where H_v is the enthalpy of formation of a hole with the size of the smallest atom. The hole enthalpy can easily be calculated using Miedema's model [20, 21]. Recently,

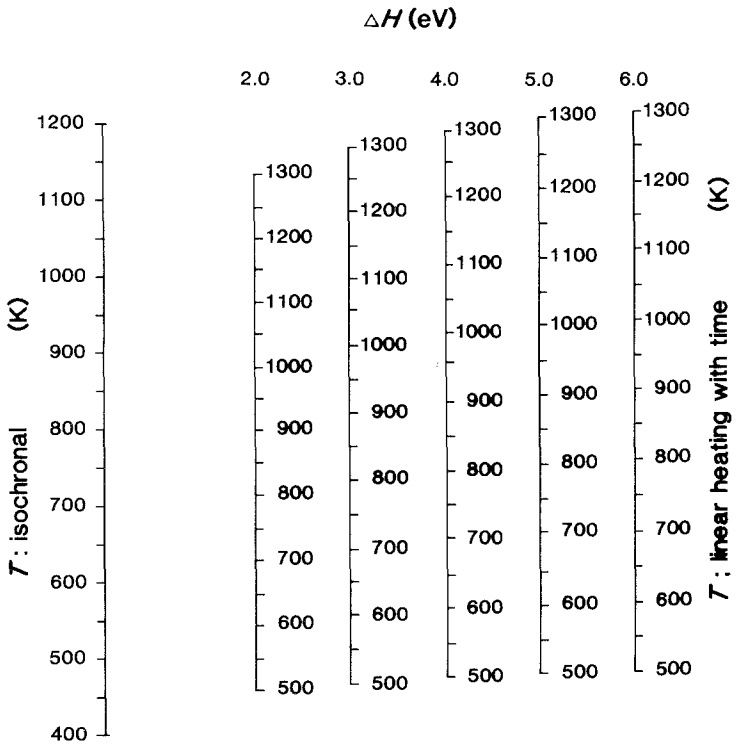

Figure 9 Diagram from which the temperature correction can be derived for a given activation energy and the two annealing schedules applied in this study. The temperature scale on the left is for isochronal annealing for 15 min and that on the right is for a linear temperature increase with time at a heating rate of 50 K min^{-1}. The intersections of the vertical bars with a horizontal line gives the temperatures for the two annealing schedules and various activation energies.

various models have appeared in the literature, which are modifications of Buschow's hole model. Weeber [8] proposed the relation $T_x = 5H_v + 275$, Barbour *et al.* [9] proposed the relation $T_x = 4.2H_{vl}$, where H_{vl} is the formation enthalpy of a hole with the size of the larger atom. A comparison with our data is not straightforward, because the models are mainly based on data derived from differential scanning calorimetry experiments with a constant heating rate of 50 K min^{-1}. In our experiments isochronal annealings were performed for 15 min, and therefore our temperatures must be corrected upwards. The magnitude of the correction depends on the activation energy. Unfortunately, due to short-range order effects [22], the activation energy can vary by almost a factor of 2 for similar crystallization temperatures. For various activation energies, the time integral of the Boltzmann factor was calculated numerically for the two annealing schedules. A diagram was constructed which is shown in Fig. 9. It was assumed that the entropy change does not depend on the temperature where crystallization occurs, but is the same for all heating schedules. The corrected crystallization temperatures and the various model values are shown in Fig. 10. Buschow's rule seems to overestimate the crystallization temperature for the studied alloys, Weeber's proposal comes closer, whereas the formula of Barbour *et al.* predicts values that are too low. The crystallization temperature for the compositions $V_{0.5}Pd_{0.5}$ and $Nb_{0.4}Pd_{0.6}$ is much lower than predicted, and is even lower than the prediction of Barbour *et al.* As correctly shown by Nastasi *et al.* [23], in those cases where crystallization takes place by polymorphic transitions, which do not require long-range diffusion, the Buschow model predicts temperatures that are much too high. Our results, showing that $V_{0.5}Pd_{0.5}$ and $Nb_{0.4}Pd_{0.6}$ crys-

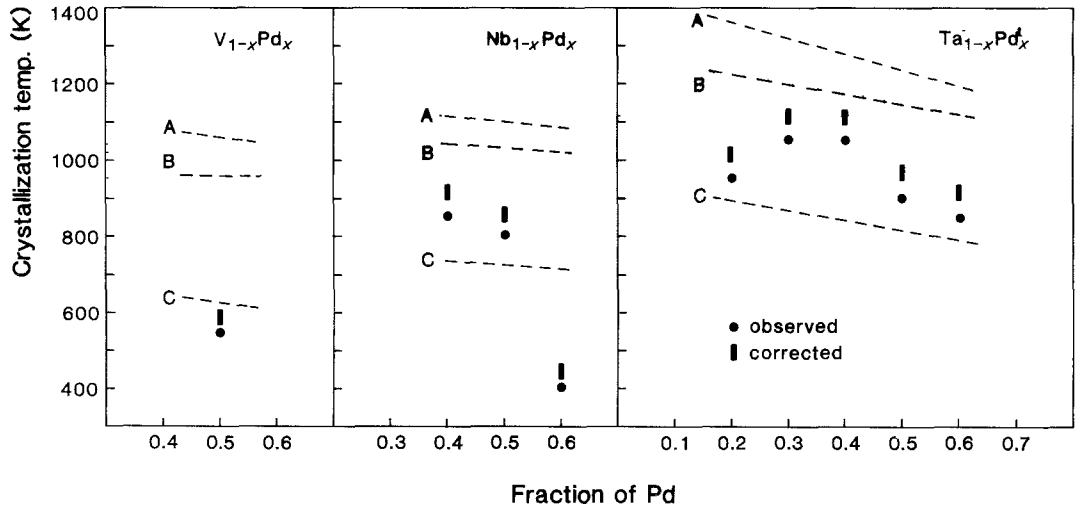

Figure 10 Observed crystallization temperatures, corrected temperatures (see Discussion), and predictions by (A) Buschow [7], (B) Weeber [8] and (C) Barbour *et al.* [9].

tallize into a single-phase fcc solid solution at a relatively low temperature, corroborate that observation.

The structures that are formed upon crystallization in the Nb–Pd system – an fcc phase and the sigma phase – are expected from the phase diagram. In the case of Ta–Pd the primary fcc crystallites that form at the crystallization temperature are metastable. The β-Ta phase that forms was also observed by Nastasi *et al.* [23] for the Ta–Cu system.

5. Conclusions

The amorphous-phase formation range in the systems V–Pd, Nb–Pd and Ta–Pd increases drastically going from 3d to 5d elements.

The compositions where solid solutions are present in the as-deposited films correspond well with the equilibrium phase diagram.

When no solid solutions are formed, the films are amorphous; the quench rate is so high that both two-phase systems and complex structures do not form.

Primary crystallization is observed for $Nb_{1-x}Pd_x$ ($x = 0.4, 0.5$) and $Ta_{1-x}Pd_x$ ($x = 0.2$ to 0.6); for all compositions the first crystalline phase to form during heating is the fcc phase. The observed crystallization temperature agrees reasonably with Buschow's hole model and modifications of that model, except for the compositions $V_{0.5}Pd_{0.5}$ and $Nb_{0.4}Pd_{0.6}$. In those cases, crystallization takes place at a lower temperature; the transition is polymorphic to a single-phase solid solution. The Buschow hole model is only valid for transitions where a certain degree of diffusion is required, which is not the case for the polymorphic transitions.

Acknowledgements

We thank H. C. Donkersloot and J. M. Kerkhof for the preparation of the specimens, and Drs Miedema and Coehoorn for stimulating the discussion.

References

1. J. S. CANTRELL, J. E. WAGNER and R. C. BOWMAN, Jr *J. Appl. Phys.* **57** (1985) 545.
2. Y. WASEDA, "The Structure of Non-Crystalline Materials" (McGraw-Hill, New York, 1980).
3. Y. SAKURAI, I. KANAZAWA, Y. WATANABE and T. IWASHITA, *J. Phys. F* **16** (1986) L265.
4. N. SAUNDERS and A. P. MIODOWNIK, *Calphad* **9** (1985) 283.
5. M. M. COLLVER and R. H. HAMMOND, *J. Appl. Phys.* **49** (1978) 2420.
6. J. J. VAN DEN BROEK and A. G. DIRKS, *Philips Technol. Rev.* **43** (1987) 304.
7. K. H. J. BUSCHOW, *Solid State Commun.* **43** (1982) 171.
8. A. W. WEEBER, *J. Phys. F* **17** (1987) 809.
9. J. C. BARBOUR, R. DE REUS, A. W. DENIER VAN DER GON and F. W. SARIS, *J. Mater. Res.* **2** (1987) 168.
10. T. MINEMURA, G. J. VAN DER KOLK and J. J. VAN DEN BROEK, *J. Less Common Metals* to be published.
11. P. DUWEZ, *Trans. Metall. Soc.* **60** (1967) 607.
12. G. DAS, *Thin Solid Films* **12** (1972) 305.
13. P. T. MOSELEY and C. J. SEABROOK, *Acta Crystallogr.* **B29** (1973) 1170.
14. K. SAMWER, *Phys. Rep.* **161** (1988) 1.
15. T. E. HUTCHINSON, *J. Appl. Phys.* **36** (1965) 270.
16. P. N. DENBIGH and R. B. MARCUS, *ibid.* **37** (1966) 4325.
17. R. COEHOORN, G. J. VAN DER KOLK, J. J. VAN DEN BROEK, T. MINEMURA and A. R. MIEDEMA, *J. Less-Common Metals* **140** (1988) 307.
18. R. E. WATSON and L. H. BENNETT, *Scripta Metall.* **17** (1983) 827.
19. U. KÖSTER, *Z. Metallkde* **75** (1984) 693.
20. K. H. J. BUSCHOW and N. M. BEEKMANS, *Solid State Commun.* **35** (1980) 233.
21. A. R. MIEDEMA, *Z. Metallkde* **70** (1979) 345.
22. K. H. J. BUSCHOW, *J. Appl. Phys.* **56** (1984) 304.
23. M. NASTASI, F. W. SARIS, L. S. HUNG and J. W. MAYER, *J. Appl. Phys.* **58** (1985) 3052.

Received 28 March
and accepted 29 July 1988